Proceedings of the Sixth International Conference on
Railway Technology: Research, Development and Maintenance
Edited by: J. Pombo
Civil-Comp Conferences, Volume 7, Paper 5.17
Civil-Comp Press, Edinburgh, United Kingdom, 2024
ISSN: 2753-3239, doi: 10.4203/ccc.7.5.17

Calculation of the Influence of the Track System on the Dynamic Behaviour of a Rolling Wheelset using a Finite Element Model

R. Benkreif, W. Daves and J. Maierhofer

**Materials Center Leoben Forschung GmbH, Leoben
Austria**

Abstract

An explicit 3D finite element model of a comprehensive railway track is established. Using this model, a study is performed which focuses on supported track systems. Within the model variations in the stiffness of rail pads and under sleeper pads are investigated which induce changes in vertical forces acting on the rail surface and influences the wheelset movement. By applying an angle of attack to the wheelset the lateral forces are influenced and calculated. Using varying track parameters, the impact of rail pad stiffness, under sleeper pad stiffness, and angle of attack on critical variables such as maximum contact pressure, vertical and lateral forces and displacements is shown. This theoretical understanding facilitates an optimized design of the track system and its interacting parameters.

Keywords: finite element model, track system, track stiffness, rail pad, under sleeper pad, angle of attack.

1 Introduction

The operation of railways is challenging due to high competition with other forms of transports. High costs arise regarding repairs and maintenance of the rail system and they have a high share of the total operational costs. Most of repairs comes from wheel or rail reprofiling, wear, out of round wheels or rail corrugation and other wheel-rail surface defects. There are several aspects for wheel and rail damage especially the dynamic behaviour of the train-track system and the operational conditions [1], [2]. Fault diagnosis have a major role in monitoring railway conditions.

Time maintenance costs, could be saved by an early diagnosis of the emerging faults. The main aim of track monitoring is to detect possible causes of defect before they cause any failure or prevent rail operation [3].

In wheel-rail damage simulations, the main problem is the wide range of time and length scale. Dynamic simulations using multi-body system software can cover length of hundreds of kilometres using fast contact calculation models which are accurate enough to regard the tribological parameters like contact patch size, distribution of pressure and shear stresses, creepage and sliding. Most models proved itself in predicting the wheel-rail damage correctly, but, there are problems beyond the accuracy of the model itself from the end user perspective [1].

Over the years many models have been introduced to study the rail track damage [4]. Zhu at al. 2013 made 3D finite element model to study the interface damage resulted among prefabricated slab and cement asphalt mortar layer. As a result the model was capable of predicting the cracks initiation and growth [5]. Another study investigates the initiation of damage in concrete in slab tracks [6]. The influence of random track irregularities on fatigue damage of fastening clips is published in [7].

The rail track system developed over the years and many elements were added to enhance its performance. During the train movement, the vehicle-track interaction causes high impact loads and thus fatigue and degradation of vehicle components and rail infrastructure. Pads are used below the rails and the sleepers to give flexibility to the track and to damp the transmission of vibrations and noise. The rail pad is responsible for the flexibility of the infrastructure [8]. Stiffness of the rail pad has impact on the track performance which was mentioned in a study that investigated the influence of rail pad stiffness on rail corrugation [9]. A study about the influence of the rail pad stiffness on vehicle-track interaction and corrugation growth is presented in [10]. A rail pad is usually made from a polymetric compound, rubber, or composite material. In most cases, dynamic responses of the railway tracks are involved directly with noise and wear phenomena in railway track environment. The exciting numerical models or simulations of railways tracks mostly exclude the influence of preloading on the nonlinear dynamic behaviour of rail. The effect of dynamic rail pad characteristics and its influence on the dynamic response of railway tracks is shown in [11].

Under sleeper pads are elements attached beneath the surface of sleepers to give an intermediate elastic layer between the sleeper and ballast. The under-sleeper pads are usually made of polyurethane elastomer with foam structure with encapsulated air voids. The main reason of installing under sleeper pad is to decrease ground vibrations and to reduce ballast damage. After investigation on the effect of under sleeper pad on dynamic train track interaction, results indicated that the effect of the under sleeper pad on train track interaction is remarkable mainly in the frequency range 0-150 Hz [12]. Under-sleeper pads reduces the stresses transmitted to the ballast and the underlying layers and reduces the size of deformation and degradation of ballast [13]. An analysis of the effect of under sleeper pads on the railway vehicle-track dynamic interaction in a transition zone was made in [14]. Using a 3D finite element model of prestressed concrete sleepers with under sleeper pads was made in [15]. That under-sleeper pads can enhance the performance of ballast under cyclic load is shown in [16].

Investigations about the angle of attack are presented in [17], [18]. Measurement methods for the angle of attack of wheelsets in curves are presented in [19]. An experimental study on the influence of friction modifiers on wheel-rail dynamic interaction with different angle of attacks was made in [20].

2 Finite Element Model

The objective of this study was to develop a finite element model to simulate the behavior of a rail-wheel system under operational conditions. For the model the commercial software ABAQUS/Explicit is used. The model contains the components that are considered essential for describing of the railway infrastructure. The vehicles are represented simplified by an axle and two wheels. The used wheel profiles are S1002, and the rails are modelled with 60E1 profiles. The geometry of the wheel axle is modeled as continuum with steel properties To ensure an accurate representation of contact interactions, the mesh size at the contact region between wheels and rails is set to 1.5 x 1.5 mm. The wheelset moves in the model over a running distance of 4000 mm on straight rails. The vehicle weight is applied via forces acting at the center of each wheel. Due to the use of continuum elements for the axle and the wheels, the masses rotational inertia, and deformation behavior of both are regarded, the weight of the bogie is simulated through a force and the primary suspension is applied using a spring-damper system. The mechanical system is sketched in Figure 1.

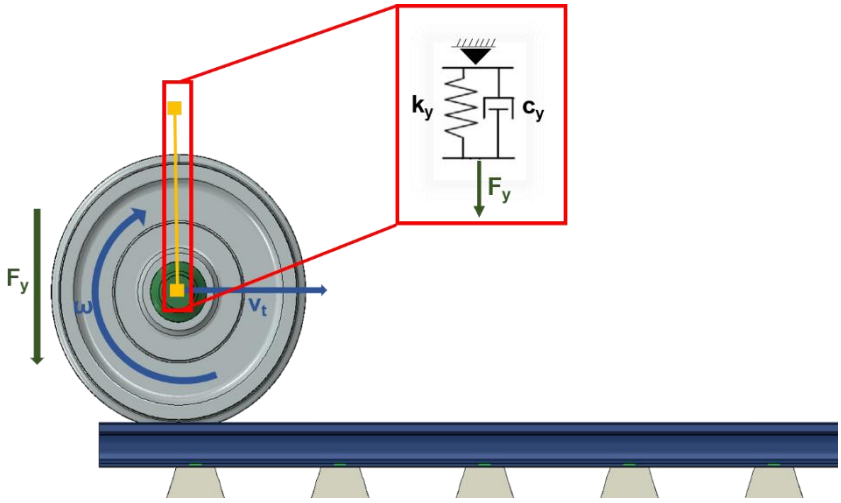

Figure 1 Kinematic model of the wheel suspension.

Because clips are seen as an important part of the rail fastening system, they are modelled with a predetermined preload using a spring. The elements representing the area where the clips are pressed onto the rail foot are fixed in both longitudinal and lateral axes, allowing movement solely in the vertical direction.
Below the rails, rail pads (ZW700) and below the sleepers under sleeper pads are used representing polyurethane-based materials. The rail pads are connected to both the rail and sleeper through tie connections, while the under-sleeper pads are connected through tie connections with the ballast and the sleepers. The ballast is modeled as

continuum with a given elastic modulus to represent a predefined stiffness varying along the length of the sleeper, see Figure 2.

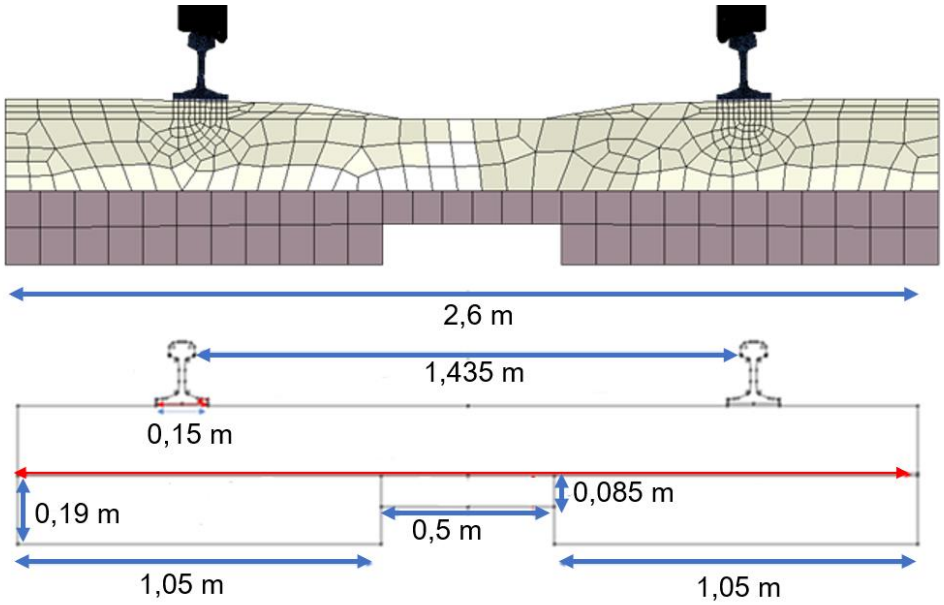

Figure 2 Geometrical setup of the ballast.

At the end of the modeled rails symmetry conditions are taken as boundaries. The Figure 1 represent the FE model used for this investigation. The parameters of the model are shown in table 1.

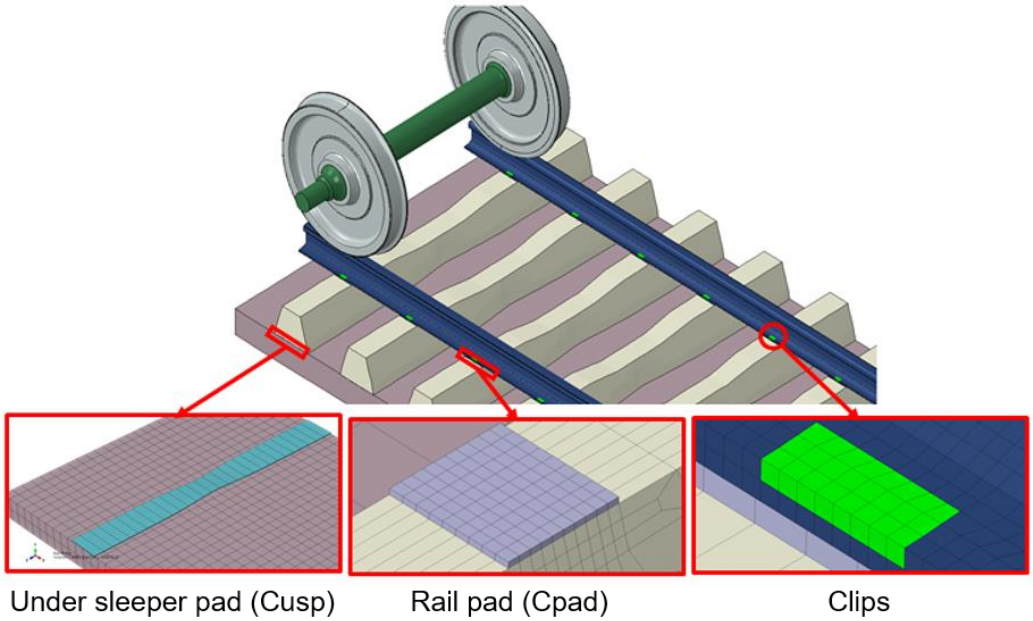

Figure 3: Illustration of straight railway system.

Parameters	Unit	Value
Rail profile	-	60E1
Rail density	kg m^{-3}	7800
Young's modulus of rail	GPa	210
Sleeper density	kg m^{-3}	2510
Young's modulus sleeper	GPa	33
Sleeper spacing	m	0.6
Length of sleeper	m	2.6
Mass of sleepers	kg	320
Length of Track	m	6.2
Track gauge	m	1.435
Wheelset load	kN	220
Train speed	km h^{-1}	120
Static wheel load	N	110000
Primary suspension stiffness	N/m	1220000
Primary suspension damping	N.s/m	30000
Clip preload	N	9000
Clip stiffness	N/m	700000
Ballast stiffness centre	N/mm³	0.1
Ballast stiffness sides	N/mm³	0.2

Table 1: Parameters used for the FE model.

3 Results

In this study, the influence of three track parameters on the dynamical behaviour of a rolling wheelset is investigated. The three parameters are the stiffness of the rail pads, the stiffness of the under-sleeper pad and the influence of a lateral force introduced by applying an angle of attack and holding the lateral position of the wheelset constant. The variables investigated are the vertical displacement of the wheelset, the vertical and lateral contact forces between wheels and rail.

Three different stiffness values were considered for the rail pads, namely Cpad 60 kN/mm, 200 kN/mm, and 600 kN/mm. The parameters taken for the study are presented in Table 2:

Parameters	Unit	Value		
Angle of attack	°	0	0.05	0.1
Rail pad stiffness	kN/mm	60	200	600
Bedding modulus under sleeper pad	N/mm³	0	0.15	0.3

Table 2: Variation of the parameter used for this investigation

In Figure 4 the vertical displacement of the wheelset is plotted. The wheel is put onto the rail at a distance of 0 m in the diagram. A vertical oscillation of the wheelset is excited which can be damped out by dissipative processes during rolling as e.g. by the primary suspension damper or the damping behaviour of the rail pads. The damping behaviour of the pads and the under-sleeper pads is not regarded in the model at hand. The damping of the primary suspension damper is active.

In Figure 4 the results of the simulation are shown. The red dashed vertical lines in Figure 4 represent the sleeper positions along the track. The diagram shows the vertical displacement of the wheelset while rolling two meters along the track. During applying the wheels on the rails, the pads, sleepers and ballast are compressed and move downwards and are reflected. This process introduces an oscillation into the whole system as can be seen in figure 4. Usually such oscillations will fade out due to the system relevant damping features as described above. To see the pure stiffness influence of pad and under-sleeper pad, damping effects are neglected.

The result in Figure 4 show, that the rail pad stiffness influences the amplitude and the wavelength and frequency of the vertical wheelset displacement. The simulations show that a rail pad stiffness of 600 kN/mm results in lower vertical wheelset displacement compared to a stiffness of 60 kN/mm. On other hand, the rail pad stiffness of 60 kN/mm exhibited higher vertical wheelset displacement which also influences the wavelength and thus the frequency of the vertical oscillation of the wheelset. This oscillation is influenced by the sleeper mass, the ballast stiffness but also significantly from the pad stiffness.

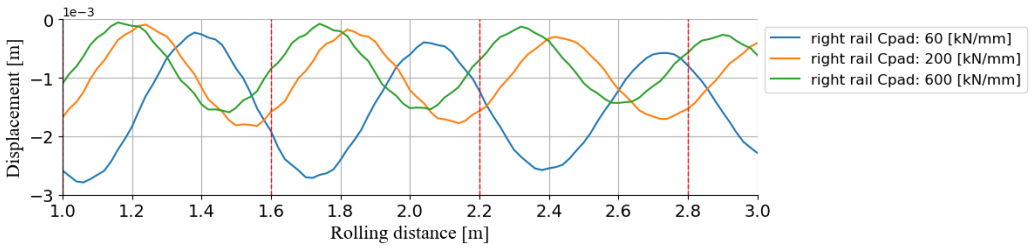

Figure 4: Vertical displacement of the wheelset.

Figure 5 shows the vertical contact forces between the wheels and the rail. Without using an angle of attack, introducing lateral forces or applying the wheelset shifted relative to the centre of the track, the results for the left and right wheel remains the same. Therefore, the contact forces for only one wheel-rail interaction are shown.

The vertical contact forces show naturally the same wavelength as the vertical wheel displacement but in contrary to the displacement they are oscillating around the static load of 110 kN with similar amplitude. This means the rail pad stiffness only slightly influences the contact forces. A remarkable influence of the rail pad stiffness can be seen in the position of the maximum forces. While for a stiffness of 200 kN/mm the maximum contact force seems to be correlated with the wheel position above the sleeper, the other stiffnesses shift the maximum away from this position due to change

of the wavelength. The lateral forces of the left and right rails are represented in Figure 6.

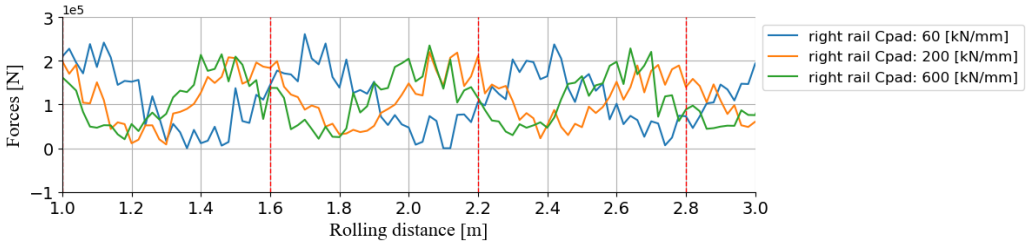

Figure 5: Vertical force on the rail surface.

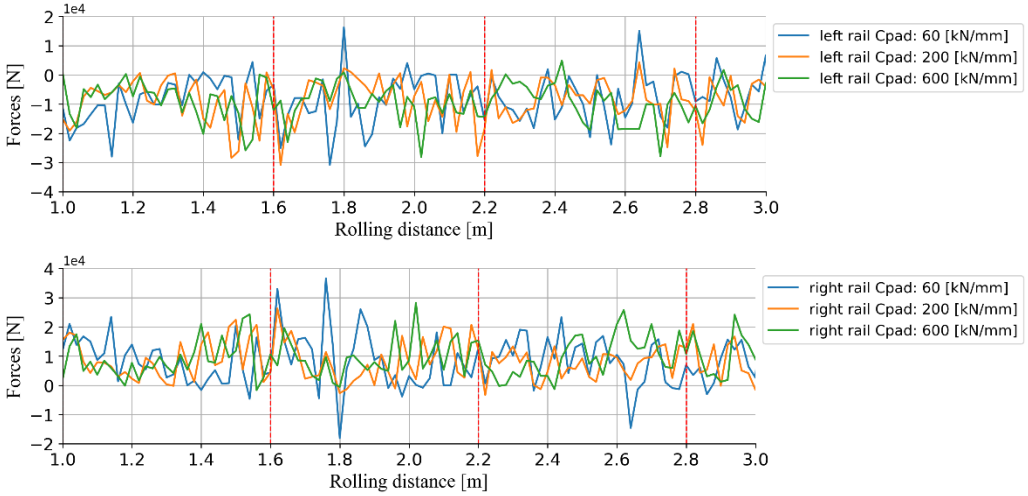

Figure 6: Lateral force on the rail surface.

Figure 7, presents the FE simulation results for a high-load case, highlighting the contact pressure (cpress) as well as the parameters cslip1 and cslip2. For this simulation, the rail pad stiffness was set to 600 kN/mm. Notably, no under-sleeper pad was used, and the angle of attack was not considered.

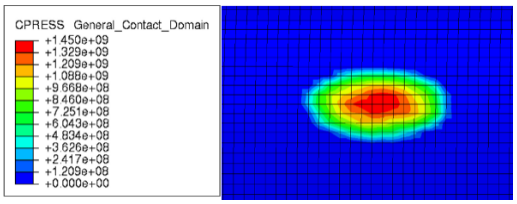

Figure 7: Plot of the wheel rail contact pressure with 600 kN/mm used for rail pad stiffness, without considering under sleeper pad and angle of attack.

In Figure 8, the vertical displacement of the wheelset is shown varying the under-sleeper pad stiffness. The result in Figure 8 shows that the stiffness of the under-sleeper pad has an effect similar to that of the rail pad, as shown in Figure 4. According to the simulations, an under-sleeper pad stiffness of 0 N/mm³ (which means there is no under sleeper pad) results in lower vertical wheelset displacement. Conversely, an

under-sleeper pad stiffness of 0.15 N/mm³ leads to higher vertical wheelset displacement. This increased displacement also affects the wavelength and, consequently, the frequency of the wheelset's vertical oscillation.

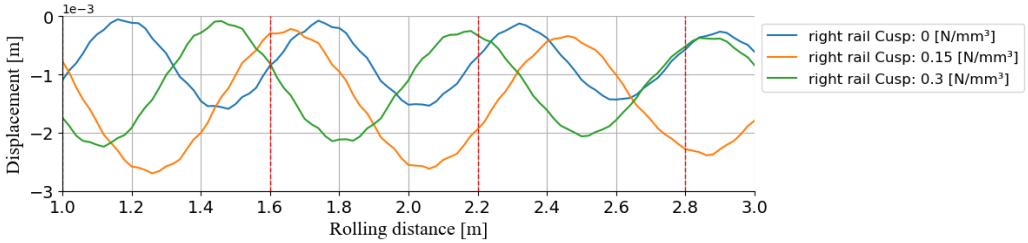

Figure 8: Vertical displacement of the wheelset.

The results shown in Figure 9 are similar to those of rail pad stiffness illustrated in Figure 5. This indicates that under sleeper pad stiffness also has a minimal effect on the contact forces. However, a notable influence of under sleeper pad stiffness is shown in the location of the maximum forces. The maximum contact forces aligns with the wheel position above the first sleeper, and due to changes in the wavelength, the maximum contact force is shifted. Figure 10 shows the results of the lateral forces of the left and right rails.

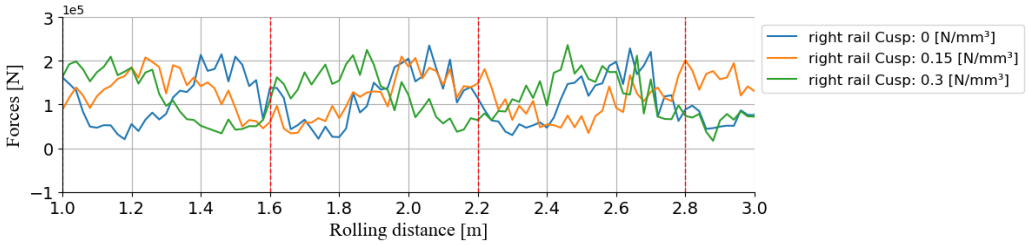

Figure 9: Vertical force on the rail surface.

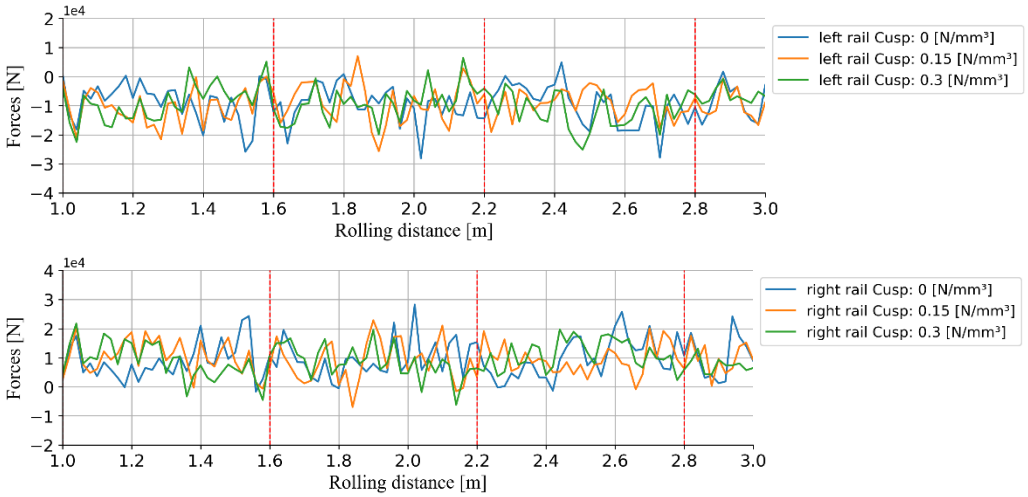

Figure 10: Lateral force on the rail surface.

In Figure 11, the vertical displacement of the wheelset is shown in dependency of the applied angel of attack of the axle. The angle of attack has no influence on the wavelength and frequency of the vertical wheelset displacement, although it may cause a slight change in amplitude. The simulations show that a 0.1° angle of attack leads to lower amplitude compared to no angle of attack considered.

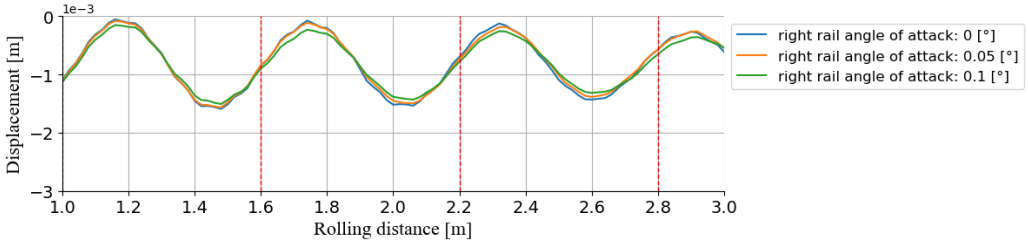

Figure 11: Vertical displacement of the wheelset.

Figure 12 shows the vertical contact forces between the wheels and the rail in dependency of the applied angle of attack. Similar to the results of the rail pad stiffness, the vertical contact forces show naturally the same amplitude and wavelength as the vertical wheel displacement. This means the angle of attack has no influences on the vertical contact forces. In contrary to rail pad stiffness results or under sleeper pad results, the maximum contact force seems to be correlated with the wheel position above the start of sleeper. Figure 13 shows the results of the lateral forces of the left and right rails

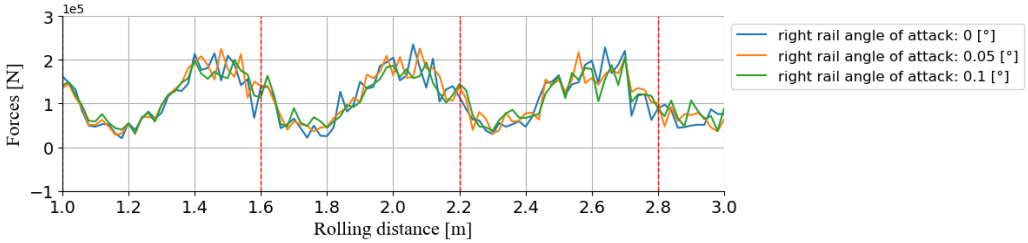

Figure 12: Vertical force on the rail surface.

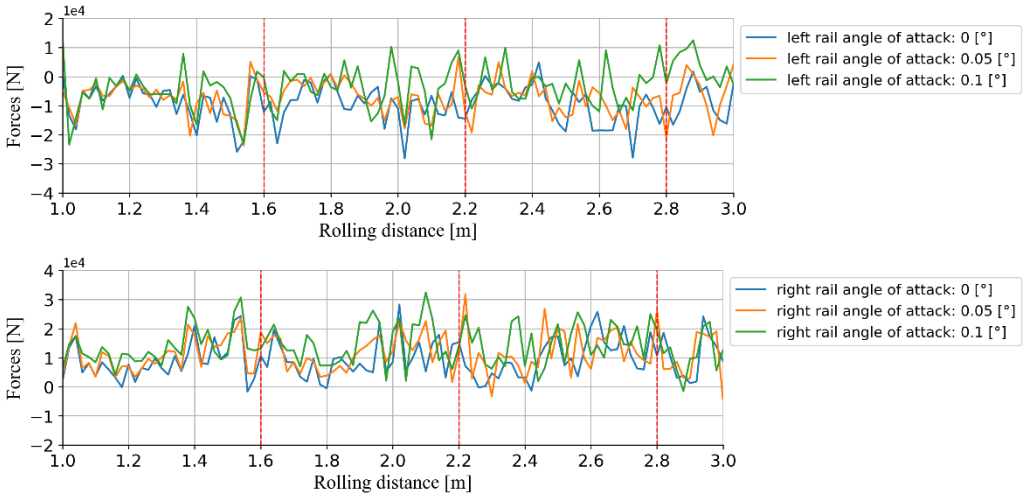

Figure 13: Lateral force on the rail surface.

4 Conclusions and Contributions

In summary, our study points out the significant impact of the rail pad and under sleeper pad on the maximum contact pressure acting on the rail surface in railway track system.

- Applying an angle of attack to the wheelset produces oscillating lateral forces on the rail surface.
- Rail pad stiffness and under-sleeper pad stiffness determines the amplitude and wavelength of vertical oscillations during the wheelset run.

Only a near to complete model of the track system is able to regard these influencing factors. Regarding such factors in railway design and maintenance will allow to design a track with optimized stiffness and damping values and will help to ensure track stability and safety.

Acknowledgements

The authors gratefully acknowledge the financial support under the scope of the COMET program within the K2 Center "Inegrated ComputationalMaterial, Process and Product Engineering (IC-MPPE)" (Project No 859480). This program is supported by the Austrian Federal Ministries for Climat Action, Environment, Energy, Mobility, Innovation and Technology (BMK) and for Digital and Economic Affairs (BMDW). Represented by the Austrian research funding association (FFG), and the federal states of Styria, Upper Austria and Tyrol.

References

[1] [1]D. Chelidze, J. P. Cusumano, and A. Chatterjee, "A dynamical systems approach to damage evolution tracking, part 1: description and experimental application," *J Vib Acoust*, vol. 124, no. 2, pp. 250–257, 2002.

[2] [2]C. Casanueva, R. Enblom, S. Stichel, and M. Berg, "On integrated wheel and track damage prediction using vehicle–track dynamic simulations," *Proc. Inst. Mech. Eng. Part F J. Rail Rapid Transit*, vol. 231, no. 7, pp. 775–785, 2017.

[3] [3]A. A. Shah, N. A. Bhatti, K. Dev, and B. S. Chowdhry, "MUHAFIZ: IoT-based track recording vehicle for the damage analysis of the railway track," *IEEE Internet Things J.*, vol. 8, no. 11, pp. 9397–9406, 2021.

[4] [4]X. Cui and X. Ling, "Effects of differential subgrade settlement on damage distribution and mechanical properties of CRTS II slab track," *Constr. Build. Mater.*, vol. 271, p. 121821, 2021.

[5] [5]S. Zhu and C. Cai, "Interface damage and its effect on vibrations of slab track under temperature and vehicle dynamic loads," *Int. J. Non-Linear Mech.*, vol. 58, pp. 222–232, 2014.

[6] [6]S. Zhu *et al.*, "Mechanical property and damage evolution of concrete interface of ballastless track in high-speed railway: Experiment and simulation," *Constr. Build. Mater.*, vol. 187, pp. 460–473, 2018.

[7] [7]D. Ma, J. Shi, Z. Yan, and L. Sun, "Failure analysis of fatigue damage for fastening clips in the ballastless track of high-speed railway considering random track irregularities," *Eng. Fail. Anal.*, vol. 131, p. 105897, 2022.

[8] [8]J. A. Sainz-Aja, I. A. Carrascal, D. Ferreño, J. Pombo, J. A. Casado, and S. Diego, “Influence of the operational conditions on static and dynamic stiffness of rail pads,” *Mech. Mater.*, vol. 148, p. 103505, 2020.

[9] [9]J. I. Egana, J. Vinolas, and M. Seco, “Investigation of the influence of rail pad stiffness on rail corrugation on a transit system,” *Wear*, vol. 261, no. 2, pp. 216–224, 2006.

[10] [10] H. Ilias, “The influence of railpad stiffness on wheelset/track interaction and corrugation growth,” *J. Sound Vib.*, vol. 227, no. 5, pp. 935–948, 1999.

[11] [11] S. Kaewunruen and A. M. Remennikov, “An alternative rail pad tester for measuring dynamic properties of rail pads under large preloads,” *Exp. Mech.*, vol. 48, pp. 55–64, 2008.

[12] [12] A. Johansson, J. C. Nielsen, R. Bolmsvik, A. Karlström, and R. Lundén, “Under sleeper pads—Influence on dynamic train–track interaction,” *Wear*, vol. 265, no. 9–10, pp. 1479–1487, 2008.

[13] [13] S. K. Navaratnarajah, B. Indraratna, and N. T. Ngo, “Influence of under sleeper pads on ballast behavior under cyclic loading: experimental and numerical studies,” *J. Geotech. Geoenvironmental Eng.*, vol. 144, no. 9, p. 04018068, 2018.

[14] [14] R. Insa, P. Salvador, J. Inarejos, and A. Roda, “Analysis of the influence of under sleeper pads on the railway vehicle/track dynamic interaction in transition zones,” *Proc. Inst. Mech. Eng. Part F J. Rail Rapid Transit*, vol. 226, no. 4, pp. 409–420, 2012.

[15] [15] C. Ngamkhanong and S. Kaewunruen, “Effects of under sleeper pads on dynamic responses of railway prestressed concrete sleepers subjected to high intensity impact loads,” *Eng. Struct.*, vol. 214, p. 110604, 2020.

[16] [16] C. Jayasuriya, B. Indraratna, and T. N. Ngo, “Experimental study to examine the role of under sleeper pads for improved performance of ballast under cyclic loading,” *Transp. Geotech.*, vol. 19, pp. 61–73, 2019.

[17] [17] T. Lack, J. Gerlici, and P. Šťastniak, “Wheelset/rail geometric characteristics and contact forces assessment with regard to angle of attack,” in *MATEC Web of Conferences*, EDP Sciences, 2019, p. 01014.

[18] [18] S. Kumar and D. P. Rao, “Wheel-rail contact wear, work, and lateral force for zero angle of attack—A laboratory study,” 1984.

[19] [19] M. Miyamoto, H. Fujimoto, T. Okabe, and E. Sato, “New measuring methods for wheelset angle of attack of railway vehicle on curves,” *JSME Int. J. Ser C Dyn. Control Robot. Des. Manuf.*, vol. 37, no. 2, pp. 292–299, 1994.

[20] [20] Z. Yang, P. Zhang, J. Moraal, and Z. Li, “An experimental study on the effects of friction modifiers on wheel–rail dynamic interactions with various angles of attack,” *Railw. Eng. Sci.*, vol. 30, no. 3, pp. 360–382, 2022.